

The role of native defects in the transport of charge and mass and the decomposition of $\text{Li}_4\text{BN}_3\text{H}_{10}$

Khang Hoang,¹ Anderson Janotti,² and Chris G. Van de Walle²

¹*Center for Computationally Assisted Science and Technology,
North Dakota State University, Fargo, ND 58108, USA.*

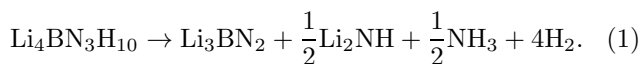
²*Materials Department, University of California, Santa Barbara, California 93106, USA.*

$\text{Li}_4\text{BN}_3\text{H}_{10}$ is of great interest for hydrogen storage and for lithium-ion battery solid electrolytes because of its high hydrogen content and high lithium-ion conductivity, respectively. The practical hydrogen storage application of this complex hydride is, however, limited due to irreversibility and cogeneration of ammonia (NH_3) during the decomposition. We report a first-principles density-functional theory study of native point defects and defect complexes in $\text{Li}_4\text{BN}_3\text{H}_{10}$, and propose an atomistic mechanism for the material's decomposition that involves mass transport mediated by native defects. In light of this specific mechanism, we argue that the release of NH_3 is associated with the formation and migration of negatively charged hydrogen vacancies inside the material, and it can be manipulated by the incorporation of suitable electrically active impurities. We also find that $\text{Li}_4\text{BN}_3\text{H}_{10}$ is prone to Frenkel disorder on the Li sublattice; lithium vacancies and interstitials are highly mobile and play an important role in mass transport and ionic conduction.

I. INTRODUCTION

The ability to store hydrogen for subsequent use is key to a hydrogen economy where hydrogen serves as an energy carrier in a carbon-neutral energy system.¹ Complex hydrides such as $\text{Li}_4\text{BN}_3\text{H}_{10}$ have been considered for hydrogen storage because of their high theoretical hydrogen density.² $\text{Li}_4\text{BN}_3\text{H}_{10}$, which is synthesized from mixtures of LiBH_4 and LiNH_2 in a 3:1 molar ratio, releases greater than 10 wt% hydrogen when heated.³ Yet its practical application is limited due to the cogeneration of ammonia (NH_3) and the irreversibility of the decomposition reaction.^{4,5} It has also been reported that metal additives such as NiCl_2 , Pd (or PdCl_2), and Pt (or PtCl_2) can suppress the release of NH_3 gas from $\text{Li}_4\text{BN}_3\text{H}_{10}$ and lower the dehydrogenation temperature;^{4,6} however, the role of these additives is still not well understood. In addition to hydrogen storage, $\text{Li}_4\text{BN}_3\text{H}_{10}$ has also shown promise as a battery solid electrolyte due to its high lithium-ion conductivity.⁷ The material was reported to have a conductivity of 2×10^{-4} S/cm at room temperature and an activation energy of 0.26 eV.⁸

The decomposition of $\text{Li}_4\text{BN}_3\text{H}_{10}$ can proceed as^{3,9}



While other reaction pathways have been proposed,^{9,10} reaction (1) whose products contain 8.9 and 9.4 mass % of H_2 and NH_3 is considered to be closest to the experimental situation where the values of 9.6 and 8.4 mass %, respectively, have been observed.^{3,9} The decomposition and dehydrogenation of $\text{Li}_4\text{BN}_3\text{H}_{10}$, like those of other complex hydrides such as LiBH_4 and LiNH_2 , necessarily involves the breaking and forming of chemical bonds and the transport of mass in the bulk. These are electronic and atomistic processes that can be fruitfully studied using first-principles calculations.^{11–16} Comprehensive and systematic computational studies of the structure, energetics, and migration of native point defects and defect

complexes can provide direct insights into the mechanisms for decomposition and dehydrogenation, help in identifying the rate-limiting processes, and ultimately aid in design of materials with improved hydrogen desorption kinetics.

Native point defects in $\text{Li}_4\text{BN}_3\text{H}_{10}$ were first studied by us based on density-functional theory (DFT);¹⁷ however only hydrogen-related defects were considered. A more comprehensive study was carried out by Farrell and Wolverton;¹⁸ they reported not only results for hydrogen vacancies and interstitials but also for some lithium-, boron-, and nitrogen-related defects. They also studied the dependence of defect formation energies on the atomic chemical potentials. Farrell and Wolverton,¹⁸ however, considered neither defect complexes nor migration of the native defects that may play an important role in mass and charge transport in the material. As reported in previous work,^{12,16,19} Frenkel defect pairs, i.e., interstitial-vacancy complexes of the same species, can play an essential role in decomposition and dehydrogenation processes.

Here we report a comprehensive and systematic DFT study of the structure, energetics, and migration of hydrogen-, lithium-, boron-, and nitrogen-related isolated native point defects in all the possible charge states, as well as defect complexes in $\text{Li}_4\text{BN}_3\text{H}_{10}$. Some results for hydrogen-related defects were reported previously,¹⁷ but are included here after applying finite-size effect corrections to the formation energy of charged hydrogen vacancies and interstitials (see details in Sec. 2); a lower energy configuration of the neutral hydrogen interstitial is also reported. We find that $\text{Li}_4\text{BN}_3\text{H}_{10}$ is prone to Frenkel disorder on the Li sublattice, and the lithium vacancies and interstitials are highly mobile and can play an important role in mass transport and ionic conduction. On the basis of our results, we propose a specific mechanism for the decomposition of $\text{Li}_4\text{BN}_3\text{H}_{10}$ in which the release of NH_3 is associated with the formation and migration of negatively charged hydrogen vacancies in

the interior of the material. In light of this mechanism, we discuss the role of transition metal impurities such as Ni, Pd, and Pt in suppressing the release of NH_3 and in lowering the dehydrogenation temperature. Comparison with previous computational studies will be made where appropriate.

II. METHODOLOGY

Our calculations are based on DFT using the generalized-gradient approximation²⁰ and the projector-augmented wave method,^{21,22} as implemented in the Vienna *Ab Initio* Simulation Package (VASP).^{23–25} We used the unit cell of $\text{Li}_4\text{BN}_3\text{H}_{10}$ containing 144 atoms and a $2 \times 2 \times 2$ Monkhorst-Pack \mathbf{k} -point mesh.²⁶ The plane-wave basis-set cutoff was set to 400 eV. Convergence with respect to self-consistent iterations was assumed when the total energy difference between cycles was less than 10^{-4} eV and the residual forces were less than 0.01 eV/Å. In the defect calculations, the lattice parameters were fixed to the calculated bulk values, but all the internal coordinates were fully relaxed. Migration was studied using the climbing-image nudged elastic band (NEB) method.²⁷

We characterize different defects in $\text{Li}_4\text{BN}_3\text{H}_{10}$ using their formation energies. Defects with low formation energies will easily form and occur in high concentrations. The formation energy of a defect X in charge state q is defined as²⁸

$$E^f(X^q) = E_{\text{tot}}(X^q) - E_{\text{tot}}(\text{bulk}) - \sum_i n_i \mu_i + q(E_v + \mu_e) + \Delta^q, \quad (2)$$

where $E_{\text{tot}}(X^q)$ and $E_{\text{tot}}(\text{bulk})$ are, respectively, the total energies of a supercell containing the defect X and of a supercell of the perfect bulk material; μ_i is the atomic chemical potential of species i (and is referenced to bulk Li metal, bulk B metal, N_2 molecules, or H_2 molecules at 0 K), and n_i denotes the number of atoms of species i that have been added ($n_i > 0$) or removed ($n_i < 0$) to form the defect. μ_e is the electronic chemical potential, i.e., the Fermi energy, referenced to the valence-band maximum in the bulk (E_v). Δ^q is the correction term to align the electrostatic potentials of the bulk and defect supercells and to account for finite-cell-size effects on the total energies of charged defects.²⁸ To correct for the finite-size effects, we adopted the Freysoldt *et al.*'s approach,^{29,30} using a static dielectric constant of 15.38 calculated using density functional perturbation theory.^{31,32} In our calculations, Δ^q can be as low as 0.05 eV for a singly charged defect or as high as 1.40 eV for a triply charged defect. We note that in Ref.¹⁷ $\Delta^q = 0$, i.e., no corrections were included in the results reported there. Farrell and Wolverton, on the other hand, took into account only the ‘‘potential alignment’’ term, reported to be of ~ 0.2 – 0.9 eV depending specific defects.¹⁸

The chemical potentials μ_i are variables and can be chosen to represent experimental situations. For defect calculations in $\text{Li}_4\text{BN}_3\text{H}_{10}$, from Eq. (1) an equilibrium

between Li_3BN_2 , Li_2NH , and $\text{Li}_4\text{BN}_3\text{H}_{10}$ can be assumed and the chemical potentials of Li, B, and N are expressed in terms of μ_{H} , which is now the only variable. In the following presentation, we set $\mu_{\text{H}} = -0.15$ eV, corresponding to the Gibbs free energy of H_2 gas at 1 bar and 282 K.³³ This condition gives $\mu_{\text{Li}} = -0.24$ eV, $\mu_{\text{B}} = -1.51$ eV, and $\mu_{\text{N}} = -1.47$ eV. With this set of chemical potentials, the calculated formation energies of the defects in $\text{Li}_4\text{BN}_3\text{H}_{10}$ are all non-negative, as shown in the next section. One can choose a different set of chemical potentials and that may affect the formation energies; however, our conclusions should not depend on the chemical potential choice. We also note that the Fermi energy μ_e is not a free parameter but subject to the charge-neutrality condition that involves all possible native defects and any impurities present in the material.²⁸

III. RESULTS

$\text{Li}_4\text{BN}_3\text{H}_{10}$ was reported to crystallize in the cubic space group $I2_13$.^{34,35} This quaternary compound can be considered as a mixture of end compounds LiBH_4 and LiNH_2 , or an ionic compound in which $(\text{Li})^+$, $(\text{NH}_2)^-$, and $(\text{BH}_4)^-$ units are the basic building blocks. The valence-band maximum (VBM) of $\text{Li}_4\text{BN}_3\text{H}_{10}$ consists of nitrogen-related unbonded states coming from the $(\text{NH}_2)^-$ units, whereas the conduction-band minimum (CBM) is composed of a mixture of N p and H s states. The electronic structure near the band-gap region is, therefore, dominated by that of LiNH_2 .^{19,36} The calculated band gap is 3.53 eV—a direct gap at the Γ point.¹⁷ Given the structural and electronic properties of $\text{Li}_4\text{BN}_3\text{H}_{10}$, one expects that native point defects in this compound will possess characteristics of those in the end compounds LiBH_4 and LiNH_2 .^{16,19,36}

A. Hydrogen-related defects

Figure 1 shows the calculated formation energies of hydrogen vacancies (V_{H}), hydrogen interstitials (H_i), and a hydrogen molecule interstitial $(\text{H}_2)_i$. Among these defects, H_i^+ and H_i^- have the lowest formation energies over a wide range of Fermi-energy values, except near their transition level, $\mu_e = 2.59$ eV, where $(\text{H}_2)_i$ has the lowest formation energy.

We find that V_{H}^0 is energetically most favorable when created by removing an H atom from a $(\text{BH}_4)^-$ unit, resulting in a trigonal planar BH_3 . Similarly, V_{H}^+ is created by removing a H atom and an extra electron from a $(\text{BH}_4)^-$ unit, forming a $\text{BH}_3\text{—H—BH}_3$ complex, i.e., two BH_4 units sharing a common H atom. V_{H}^- , on the other hand, is most energetically favorable when created by removing an H^+ ion from a $(\text{NH}_2)^-$ unit, leaving the system with a $(\text{NH})^{2-}$ unit.

For the interstitials, H_i^+ is most favorable when the added H^+ ion combines with an $(\text{NH}_2)^-$ unit to form

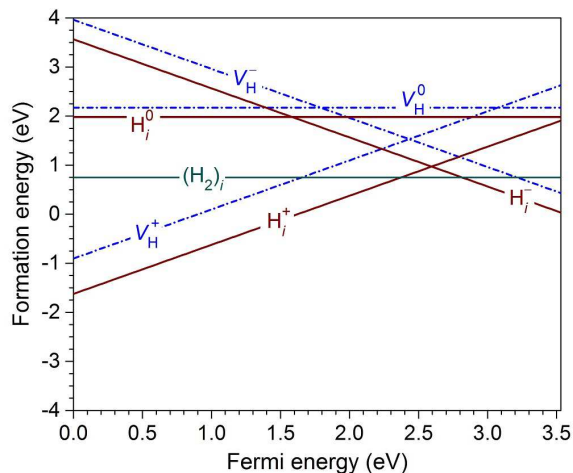


FIG. 1. Calculated formation energies of hydrogen-related defects, plotted as a function of Fermi energy with respect to the VBM.

an NH_3 unit. H_i^- , on the other hand, is found situated in a void surrounded by $(\text{Li})^+$ units. Like H_i^+ , H_i^0 also forms an NH_3 unit, which is in agreement with the configuration reported by Farrell and Wolverson,¹⁸ and is lower in energy than that reported previously by us where the neutral H atom loosely bonds to a $(\text{BH}_4)^-$ unit.¹⁷ However, even with this low-energy configuration, H_i^0 is never the most stable charge state of hydrogen interstitials. Finally, $(\text{H}_2)_i$, created by adding an H_2 molecule to the system, prefers to stay in the void formed by other species with the calculated H–H bond length being 0.76 Å, which is comparable to that of an isolated H_2 molecule (0.75 Å).

Our results thus indicate that in $\text{Li}_4\text{BN}_3\text{H}_{10}$, V_{H}^0 and V_{H}^+ possess the characteristics of those in LiBH_4 ; H_i^0 , H_i^+ , and V_{H}^- are similar to those in LiNH_2 ; and H_i^- and $(\text{H}_2)_i$ inherit their structures from those in both the end compounds.^{16,19,36}

For the diffusion of H_i^+ , H_i^- , V_{H}^+ , and V_{H}^- , we find energy barriers of 0.48, 0.49, 0.64, and 1.02 eV, respectively. The barriers for H_i^+ , V_{H}^+ , and V_{H}^- are higher because their diffusion involves breaking B–H or N–H bonds. For example, the diffusion of V_{H}^- involves moving a hydrogen atom from a nearby NH_2 unit to the vacancy. The saddle-point configuration in this case consists of a hydrogen atom located midway between two NH units, i.e., $\text{NH}-\text{H}-\text{NH}$. H_i^- , on the other hand, loosely bonds to $(\text{Li})^+$ units and therefore can diffuse more easily. For comparison, the migration barriers of H_i^+ , H_i^- , and V_{H}^- in LiNH_2 are 0.61, 0.34, and 0.71 eV,³⁶ and those of H_i^- and V_{H}^+ in LiBH_4 are 0.41 and 0.91 eV, respectively.¹⁶

Possible hydrogen-related Frenkel defect pairs are $(\text{H}_i^+, V_{\text{H}}^-)$ and $(\text{H}_i^-, V_{\text{H}}^+)$. Figure 2(a) shows the structure of $(\text{H}_i^+, V_{\text{H}}^-)$. The configurations of the individual defects are preserved in this complex, i.e., a NH_3 unit for H_i^+ and a $(\text{NH})^{2-}$ unit for V_{H}^- . The distance between the two N ions in the pair is 3.06 Å. This Frenkel pair has a

formation energy of 1.66 eV (independent of the chemical potentials), and a binding energy of 0.68 eV with respect to its isolated constituents. For comparison, a similar hydrogen Frenkel pair in LiNH_2 has a calculated formation energy of 1.54 eV.³⁶ Figure 2(b) shows the structure of $(\text{H}_i^-, V_{\text{H}}^+)$. The configurations of the individual defects are also preserved in this case. The distance from H_i^- to the H atom near the center of V_{H}^+ is 4.25 Å. This pair has a formation energy of 2.14 eV and a binding energy of 0.53 eV. The formation energy of this Frenkel pair in LiBH_4 is 2.28 eV.¹⁶

B. Lithium-related defects

Figure 3 shows the calculated formation energies of lithium vacancies (V_{Li}), interstitials (Li_i), and antisite defects (Li_i^0 , i.e., Li replacing an H atom). The creation of V_{Li}^- corresponds to the removal of a $(\text{Li})^+$ unit from the system; whereas Li_i^+ can be thought of as the addition of a Li^+ ion to the system. These two defects result in relatively small local perturbations in the $\text{Li}_4\text{BN}_3\text{H}_{10}$ lattice. The creation of Li_i^0 , on the other hand, leaves the system with an $(\text{NH})^{2-}$ unit and a Li interstitial. Thus, Li_i^0 can be regarded as a complex of Li_i^+ and V_{H}^- with a binding energy of 1.25 eV. Since the resulting defects are a $(\text{NH})^{2-}$ unit and a Li interstitial, the region that includes Li_i^0 can be considered as locally Li_2NH inside the bulk $\text{Li}_4\text{BN}_3\text{H}_{10}$. This situation is similar to Li_i^0 in LiNH_2 .³⁶

We find that Li_i^+ and V_{Li}^- have migration barriers of 0.43 and 0.20 eV, respectively. For Li_i^0 , which is considered as a complex of Li_i^+ and V_{H}^- , the lower bound of the barrier is 1.02 eV, i.e., given by the least mobile species.³⁶ For comparison, the migration barrier of Li_i^+ in LiNH_2 and LiBH_4 is 0.30 eV, and that of V_{Li}^- is 0.20 eV in LiNH_2 or 0.29 eV in LiBH_4 .^{16,19,36}

Figure 2(c) shows the structure of $(\text{Li}_i^+, V_{\text{Li}}^-)$ Frenkel pair. The distance between Li_i^+ and V_{Li}^- is 2.96 Å. $(\text{Li}_i^+, V_{\text{Li}}^-)$ has a formation energy of 0.55 eV and a binding energy of 0.58 eV. For comparison, the calculated formation energies of a similar Frenkel pair in LiNH_2 and LiBH_4 are 0.65 eV and 0.95 eV, respectively.^{16,36}

C. Boron-related defects

Figure 4 shows the calculated formation energies of V_{B} , V_{BH} , V_{BH_2} , V_{BH_3} , and V_{BH_4} in different charge states. Like in LiBH_4 ,¹⁶ the creation of $V_{\text{BH}_4}^+$ involves removing an entire $(\text{BH}_4)^-$ unit from the bulk. We find that there is very small change in the local lattice structure surrounding this defect. The structure and energetics of other boron-related defects can be interpreted in terms of $V_{\text{BH}_4}^+$ and hydrogen-related defects such as H_i^+ , H_i^- , and/or $(\text{H}_2)_i$, similar to our analysis of the defects in LiBH_4 .¹⁶ For example, $V_{\text{BH}_3}^0$ can be regarded as a com-

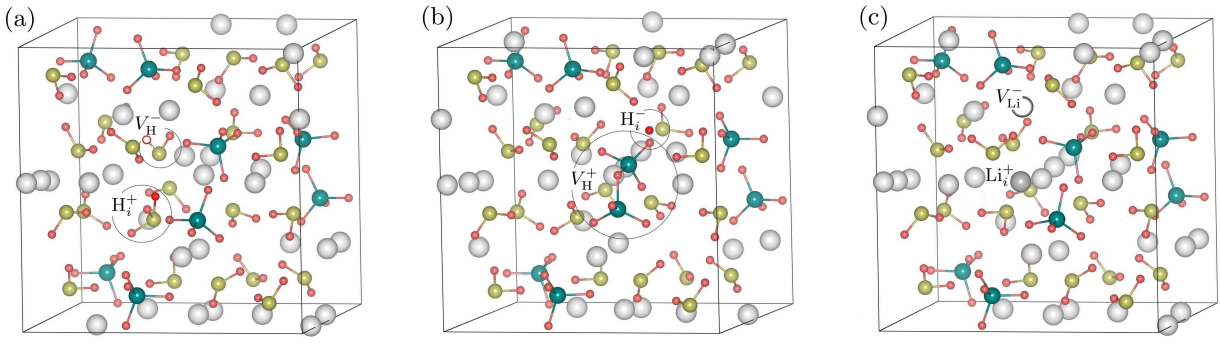


FIG. 2. Frenkel defect pairs: (a) (H_i^+, V_H^-) , (b) (H_i^-, V_H^+) , and (c) (Li_i^+, V_{Li}^-) . Large (gray) spheres are Li, medium (blue) spheres B, small (yellow) spheres N, and smaller (red) spheres H. Vacancies are represented by empty spheres.

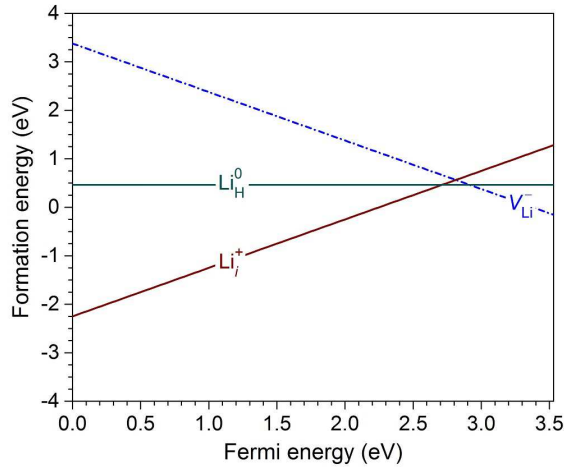


FIG. 3. Calculated formation energies of lithium-related defects, plotted as a function of Fermi energy with respect to the VBM.

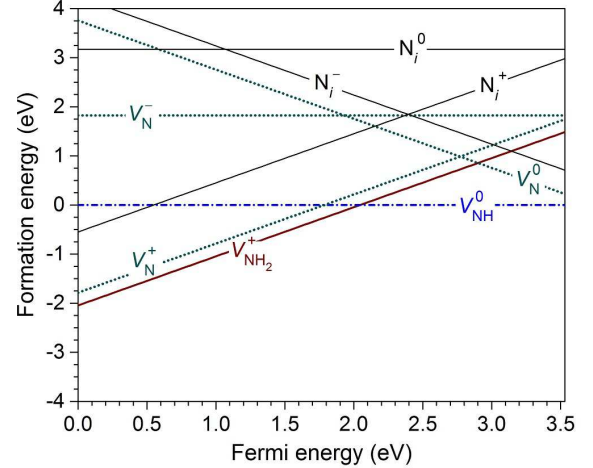


FIG. 5. Calculated formation energies of nitrogen-related defects, plotted as a function of Fermi energy with respect to the VBM.

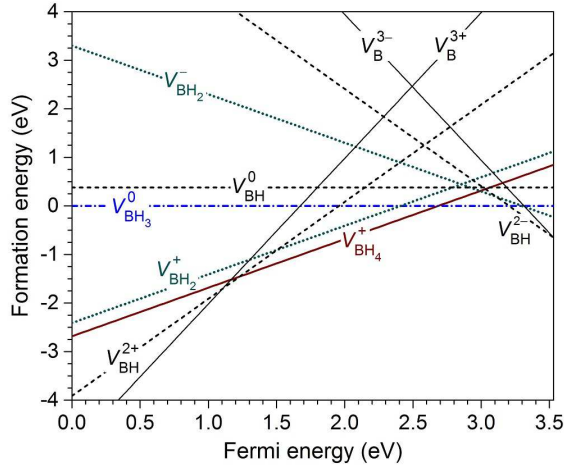


FIG. 4. Calculated formation energies of boron-related defects, plotted as a function of Fermi energy with respect to the VBM.

plex of $V_{BH_4}^+$ and H_i^- with a binding energy of 0.91 eV. Finally, the boron interstitial (B_i ; not included in Fig. 4) is most stable as B_i^- whose formation energy is 2.19 eV at $\mu_e = 2.92$ eV. The structure of B_i^- consists of a BH_2 unit and two NH units, i.e., an $HN-BH_2-NH$ complex, with the $B-N$ distance being 1.59 Å (compared to that of 1.35 Å in Li_3BN_2). Other charge states of B_i have much higher formation energies.

The migration of $V_{BH_4}^+$ involves moving a nearby $(BH_4)^-$ unit to the vacancy, with an energy barrier of 0.19 eV. For $V_{BH_3}^+$, which can be considered as a complex of $V_{BH_4}^+$ and H_i^- , the lower bound of the migration barrier is 0.49 eV. For comparison, the migration barrier of $V_{BH_4}^+$ in $LiBH_4$ is 0.27 eV.¹⁶

D. Nitrogen-related defects

Figure 5 shows the calculated formation energies of NH_2 vacancies (V_{NH_2}), NH vacancies (V_{NH}), and nitrogen vacancies (V_N) and interstitials (N_i). We find that

TABLE I. Formation energies (E^f), migration barriers (E_m), and binding energies (E_b) of selected native defects in $\text{Li}_4\text{BN}_3\text{H}_{10}$. Migration barriers denoted by an asterisk (*) are estimated by considering the defect as a complex and taking the highest of the migration barriers of the constituents.

Defect	E^f (eV)	E_m (eV)	E_b (eV)	Constituents
H_i^+	1.36	0.48		
H_i^-	0.58	0.49		
V_H^+	2.08	0.64		
V_H^-	0.98	1.02		
$(\text{H}_2)_i$	0.75			
Li_i^+	0.73	0.43		
V_Li^-	0.40	0.20		
Li_H^0	0.46	1.02*	1.25	$\text{Li}_i^+ + \text{V}_\text{H}^-$
$\text{V}_{\text{NH}_2}^+$	0.94	0.59		
V_{NH}^0	0.00	0.59*	1.53	$\text{V}_{\text{NH}_2}^+ + \text{H}_i^-$
$\text{V}_{\text{BH}_4}^+$	0.32	0.19		
V_{BH}^0	0.38		1.27	$\text{V}_{\text{BH}_4}^+ + (\text{H}_2)_i + \text{H}_i^-$
$\text{V}_{\text{BH}_2}^-$	0.32	0.49*	1.17	$\text{V}_{\text{BH}_4}^+ + 2\text{H}_i^-$
$\text{V}_{\text{BH}_3}^0$	0.00	0.49*	0.91	$\text{V}_{\text{BH}_4}^+ + \text{H}_i^-$

V_{NH_2} is energetically stable as $\text{V}_{\text{NH}_2}^+$, V_{NH} as V_{NH}^0 , V_N as V_N^+ and V_N^- , and N_i as N_i^+ and N_i^- configurations. The creation of $\text{V}_{\text{NH}_2}^+$ corresponds to the removal of an entire $(\text{NH}_2)^-$ unit from the bulk. We find that there is very small change in the local lattice structure surrounding this defect. The formation of V_{NH}^0 , on the other hand, leaves one H atom in the void left by a removed $(\text{NH}_2)^-$ unit. V_{NH}^0 can be then regarded as a complex of $\text{V}_{\text{NH}_2}^+$ and H_i^- , with a binding energy of 1.53 eV. Similarly, V_N^+ can be regarded as a complex composed of $\text{V}_{\text{NH}_2}^+$ and $(\text{H}_2)_i$, and V_N^- as a complex of $\text{V}_{\text{NH}_2}^+$ and two H_i^- defects. The structure and energetics of these nitrogen-related defects are, therefore, similar to those in LiNH_2 .³⁶ For nitrogen interstitials, the structure of N_i^0 and N_i^- consists of a BH_3 unit and an NH unit, i.e., an $\text{H}_3\text{B}-\text{NH}$ complex, with the B-N distance being 1.48 Å in N_i^0 or 1.50 Å in N_i^- . The structure of N_i^+ , on the other hand, consists of a BH_2 unit and an NH_2 unit, i.e., an $\text{H}_2\text{B}-\text{NH}_2$ complex, with the B-N distance being 1.39 Å.

The migration of $\text{V}_{\text{NH}_2}^+$ involves moving an NH_2^- unit to the vacancy, with a calculated energy barrier of 0.59 eV. For V_{NH}^0 , which can be considered as a complex of $\text{V}_{\text{NH}_2}^+$ and H_i^- , the lower bound of the migration barrier is 0.59 eV. For comparison, the migration barrier of $\text{V}_{\text{NH}_2}^+$ in LiNH_2 is 0.87 eV.³⁶

IV. DISCUSSION

We list in Table I formation energies and migration barriers of native defects and defect complexes that are most relevant to lithium-ion conduction and decomposition of $\text{Li}_4\text{BN}_3\text{H}_{10}$. The formation energies for charged defects are taken at $\mu_e = 2.92$ eV (hereafter referred to as μ_e^{int}), where the charge neutrality condition is main-

tained. This Fermi-energy position is determined by solving self-consistently the charge neutrality equation that involves the concentrations of all native (intrinsic) defects,²⁸ assuming that electrically active impurities are absent or occur with much lower concentrations than the charged native defects. In this case, it is determined exclusively by $\text{V}_{\text{BH}_4}^+$ and $\text{V}_{\text{BH}_2}^-$ (i.e., a complex of $\text{V}_{\text{BH}_4}^+$ and two H_i^-), two defects that have the lowest formation energies. For comparison, Farrell and Wolverton reported $\mu_e^{\text{int}} \sim 2.5-3.2$ eV under different sets of the atomic chemical potentials.¹⁸

It emerges from our results that some native defects in $\text{Li}_4\text{BN}_3\text{H}_{10}$ can have very low formation energies. With our choice of the atomic chemical potentials, V_{NH}^0 (a complex of $\text{V}_{\text{NH}_2}^+$ and H_i^-) and $\text{V}_{\text{BH}_3}^0$ (a complex of $\text{V}_{\text{BH}_4}^+$ and H_i^-) even have a zero formation energy. Farrell and Wolverton also found very low formation energies for these defects.¹⁸ The elementary defects $\text{V}_{\text{NH}_2}^+$, $\text{V}_{\text{BH}_4}^+$, and H_i^- that make up the neutral complexes also have low formation energies; *cf.* Table I. Overall, our results are in qualitative agreement with those reported by Farrell and Wolverton,¹⁸ and consistent with our results for native defects in LiNH_2 and LiBH_4 reported previously.^{16,19,36}

A. Lithium-ion conduction

The calculated formation energy of the $(\text{Li}_i^+, \text{V}_{\text{Li}}^-)$ Frenkel pair is only 0.55 eV, much lower than that of the hydrogen Frenkel pairs. The low formation energy of $(\text{Li}_i^+, \text{V}_{\text{Li}}^-)$ suggests that $\text{Li}_4\text{BN}_3\text{H}_{10}$ is prone to Frenkel disorder on the Li sublattice. Farrell *et al.*,³⁷ through first-principles molecular dynamics simulations, also found that the Li sublattice disorders before the anionic sublattices and the energy barrier of Li migration is ~ 0.21 eV in a temperature region above the experimental melting point. Experimentally, Matsuo *et al.*⁸ reported an activation energy of 0.26 eV for the ionic conduction in $\text{Li}_4\text{BN}_3\text{H}_{10}$ before melting. These values are very close to our calculated value (0.20 eV) for the migration barrier of V_{Li}^- . In general, the activation energy for ionic conduction is the sum of the formation energy and migration barrier, i.e., $E_a = E^f + E_m$. However, it is very likely that in the measurements of the ionic conductivity in Ref.⁸ the Li sublattice was already disordered and there were plenty of *athermal* Li vacancies and interstitials. In that case, the activation energy is dominated by the migration barrier term, i.e., $E_a \sim E_m$,³⁸ which explains why our calculated migration barrier of V_{Li}^- is comparable to the measured activation energy.

B. Decomposition mechanism

Let us now discuss the role of native defects in the decomposition of $\text{Li}_4\text{BN}_3\text{H}_{10}$. Like in LiNH_2 and LiBH_4 ,^{16,19,36} it is important to note that the decom-

position involves breaking N–H bonds in the $(\text{NH}_2)^-$ units and B–H bonds in the $(\text{BH}_4)^-$ units, which can be accomplished through the creation of relevant native defects. Besides, the process necessarily involves hydrogen, boron, and/or nitrogen mass transport in the bulk mediated by native defects; and as charged defects are migrating, local and global charge neutrality must be maintained. Finally, charge and mass conservation is required for the creation of defects in the interior of the material.

V_{H}^- , for instance, can form in the interior of the material via the $(\text{H}_i^+, V_{\text{H}}^-)$ Frenkel pair mechanism [Fig. 2(a)] in which both charge and mass are conserved, or at the surface or interface. V_{H}^+ , on the other hand, is not likely to form in the bulk because the formation energy of the $(\text{H}_i^-, V_{\text{H}}^+)$ Frenkel pair [Fig. 2(b)] is relatively high (2.14 eV), but it certainly can form at the surface or interface. $V_{\text{NH}_2}^+$ and $V_{\text{BH}_4}^+$ can only be created at the surface or interface since the creation of such defects inside the material requires creation of corresponding $(\text{NH}_2)^-$ and $(\text{BH}_4)^-$ interstitials which are too high in energy. Finally, Li_i^+ and V_{Li}^- can easily form in the bulk through the lithium Frenkel pair mechanism [Fig. 2(c)]. With their low formation energies and high mobilities, these lithium interstitial and vacancy can act as accompanying defects in mass transport, providing local charge neutrality as hydrogen-, boron-, and nitrogen-related charged defects migrating in the bulk.

Given the above considerations and the properties of the defects, $\text{Li}_4\text{BN}_3\text{H}_{10}$ decomposition can be described in terms of the following processes which may occur simultaneously:

(i) V_{H}^- is created at the surface or interface by removing an H^+ from the bulk. This H^+ ion can combine with H^- [that is liberated from $\text{Li}_4\text{BN}_3\text{H}_{10}$ when creating $V_{\text{BH}_4}^+$ via process (ii), see below] to form H_2 , or with a surface $(\text{NH}_2)^-$ unit to form NH_3 that is subsequently released or reacts with other species (see below). In order to maintain the reaction, H^+ has to be transported to the surface/interface, which is equivalent to V_{H}^- diffusing into the bulk. As V_{H}^- is migrating, local charge neutrality is maintained by the mobile Li_i^+ . These two defects can combine and form Li_{H}^0 , which is in fact a Li_2NH unit inside $\text{Li}_4\text{BN}_3\text{H}_{10}$. We note that V_{H}^- can also be created simultaneously with H_i^+ in the interior of the material through forming a $(\text{H}_i^+, V_{\text{H}}^-)$ Frenkel pair. V_{H}^- and H_i^+ then become separated as H_i^+ jumps from one $(\text{NH}_2)^-$ unit to another. This is equivalent to displacing the NH_3 unit away from the $(\text{NH})^{2-}$ unit, leaving two Li^+ next to $(\text{NH})^{2-}$, i.e., a formula unit of Li_2NH . H_i^+ then migrates to the surface/interface and is released as NH_3 . These are the same mechanisms we have proposed for the decomposition of LiNH_2 into Li_2NH and NH_3 as described in Refs.¹⁹ and³⁶. The mechanism happening at the surface/interface is expected to be dominant over the bulk mechanism since the energy required for the creation of defects inside the material is higher.

Alternatively, one starts with the creation of $V_{\text{NH}_2}^+$ at

the surface or interface by removing one $(\text{NH}_2)^-$ unit from the bulk. This unit then can combine with one hydrogen atom from a surface $(\text{NH}_2)^-$ unit and releases as NH_3 . This process also leaves $\text{Li}_4\text{BN}_3\text{H}_{10}$ with a V_{H}^- near the surface/interface. In order to maintain the reaction, $(\text{NH}_2)^-$ has to be transported to the surface/interface, which is equivalent to $V_{\text{NH}_2}^+$ diffusing into the bulk. As $V_{\text{NH}_2}^+$ is migrating, local charge neutrality is maintained by having the highly mobile V_{Li}^- in the vacancy's vicinity. The newly created V_{H}^- also needs to diffuse into the bulk. As this vacancy is migrating, local charge neutrality is maintained by the mobile Li_i^+ . These two defects can combine and form Li_{H}^0 , which is in fact a Li_2NH unit. This description is thus equivalent to the above mechanism that starts with the creation of V_{H}^- at the surface/interface. In both descriptions, the creation of V_{H}^- is crucial since it is responsible for breaking N–H bonds and turning $(\text{NH}_2)^-$ into $(\text{NH})^{2-}$.

(ii) $V_{\text{BH}_4}^+$ is created at the surface or interface by removing a $(\text{BH}_4)^-$ unit from the bulk. Since $(\text{BH}_4)^-$ is not stable outside the material, it dissociates into BH_3 and H^- where the latter stays near the surface/interface. This process is similar to that for LiBH_4 decomposition as described in Ref.¹⁶. The BH_3 unit can then combine with the NH_3 unit [that is released from the bulk through process (i)] to form ammonia borane (H_3NBH_3) or some other intermediates which subsequently release H_2 and act as nucleation sites for the formation of Li_3BN_2 . We note that the amount of NH_3 can be three times higher than that of BH_3 because the number of $(\text{NH}_2)^-$ units is three times higher than that of $(\text{BH}_4)^-$ units in $\text{Li}_4\text{BN}_3\text{H}_{10}$. From the surface/interface, H^- combines with H^+ [that is liberated from $\text{Li}_4\text{BN}_3\text{H}_{10}$ when creating V_{H}^- via process (i)] to form H_2 , or diffuses into the bulk in form of H_i^- . In the latter case, H_i^- can then combine with Li^+ to form LiH , which can be a product or an intermediate for further reactions. The hydrogen interstitial can also diffuse along with $V_{\text{BH}_4}^+$ in form of $V_{\text{BH}_3}^0$. Like in process (i) that is associated with the formation and migration of V_{H}^- , the mobile Li_i^+ and V_{Li}^- provide local charge neutrality as $V_{\text{BH}_4}^+$ and/or H_i^- are migrating in the bulk.

The rate-limiting step in (i) and (ii) is not the creation of defects at the surface or interface, but the diffusion of V_{H}^- , H_i^- , $V_{\text{NH}_2}^+$, $V_{\text{BH}_4}^+$, or $(\text{Li}_i^+, V_{\text{Li}}^-)$ inside the material, whichever defect that has the highest activation energy for formation and migration. The only assumption here is that the formation energy of these defects on the surface/interface is lower than in the bulk, which is a safe assumption given the bonding environment at the surface/interface is less constrained than in the bulk. Since these defects, except for the lithium Frenkel pair, are charged, their formation energies and hence concentrations are dependent on the Fermi-energy position. This opens the door to manipulating their concentrations and hence the decomposition kinetics through shifting the position of the Fermi energy, which can be accomplished by,

e.g., incorporating suitable electrically active impurities into the system.^{16,17}

C. Effects of metal additives

As reported previously,¹⁷ some transition-metal impurities such as Ni, Pd, and Pt can be electrically active in $\text{Li}_4\text{BN}_3\text{H}_{10}$ and effective in shifting the Fermi energy. When incorporated into $\text{Li}_4\text{BN}_3\text{H}_{10}$ at a certain lattice site with a concentration higher than that of the charged native defects, often through non-equilibrium processes such as high-energy ball milling as noted in Ref.¹⁶, these impurities determine the Fermi energy of the system and shift it to a new position (hereafter referred to as μ_e^{ext} , the Fermi-energy position determined by the extrinsic defects). Specifically, Ni can shift the Fermi energy to μ_e^{ext} at 1.91 eV (if incorporated on the B site), 2.52 eV (N site), or 1.87 eV (Li site); 1.82 eV (B site), 2.15 eV (N site), or 1.73 eV (Li site) for Pd; and 1.78 eV (B site), 2.21 eV (N site), or 1.84 eV (Li site) for Pt. Ni, Pd, and Pt are not effective in shifting the Fermi energy if incorporated at interstitial sites.¹⁷ For all these impurities, μ_e^{ext} is much lower than μ_e^{int} , i.e., the Fermi energy is shifted toward the VBM, thus lowering (increasing) the formation energy of positively (negatively) charged native defects. The incorporation of Ni, Pd, or Pt thus increases the activation energy associated with V_{H}^- , i.e., delaying the formation of NH_3 , and decreases the activation energy associated with $V_{\text{BH}_4}^+$, i.e., enhancing the formation of BH_3 and hence H_2 and/or intermediates for H_2 release and lowering the dehydrogenation temperature. Delaying the formation and subsequent release of NH_3 has important consequences: it enhances the probability of NH_3 [created in process (i)] being captured by BH_3 [created in process (ii)] or other species before being released as NH_3 gas. Our results thus explain why metal additives such as NiCl_2 , Pd (or PdCl_2), and Pt (or PtCl_2) are effective in suppressing the release of NH_3 gas

from the decomposition of $\text{Li}_4\text{BN}_3\text{H}_{10}$ and lowering the dehydrogenation temperature.

V. CONCLUSIONS

We have carried out a comprehensive first-principles study of native point defects and defect complexes in $\text{Li}_4\text{BN}_3\text{H}_{10}$. We find that lithium interstitials and vacancies are highly mobile and can be created in the interior of the material via a Frenkel pair mechanism with a low formation energy. These defects can participate in lithium-ion conduction or act as accompanying defects which provide local charge neutrality in hydrogen, boron, or nitrogen mass transport. We have proposed an atomistic mechanism for the decomposition of $\text{Li}_4\text{BN}_3\text{H}_{10}$, involving the formation and migration of V_{H}^- , H_i^- , $V_{\text{NH}_2}^+$, $V_{\text{BH}_4}^+$, and $(\text{Li}_i^+, V_{\text{Li}}^-)$ in the bulk. On the basis of this mechanism, we explain the decomposition and dehydrogenation of $\text{Li}_4\text{BN}_3\text{H}_{10}$ and the effects of metal additives on these processes and, particularly, the suppression of NH_3 release and the lowering of the dehydrogenation temperature as observed in experiments.

ACKNOWLEDGMENTS

This work was supported by the Office of Science of the U.S. Department of Energy (Grant No. DE-FG02-07ER46434) and by the Center for Computationally Assisted Science and Technology (CCASt) at North Dakota State University. High performance computing resources were provided by CCASt, the Texas Advanced Computing Center (TACC) at the University of Texas at Austin, and the National Energy Research Scientific Computing Center (NERSC), a DOE Office of Science User Facility supported by the Office of Science of the U.S. Department of Energy under Contract No. DE-AC02-05CH11231.

¹ U. Eberle, M. Felderhoff, and F. Schüth, *Angew. Chem. Int. Ed.* **48**, 6608 (2009).

² S.-i. Orimo, Y. Nakamori, J. R. Eliseo, A. Züttel, and C. M. Jensen, *Chem. Rev.* **107**, 4111 (2007).

³ G. P. Meisner, M. L. Scullin, M. P. Balogh, F. E. Pinkerton, and M. S. Meyer, *J. Phys. Chem. B* **110**, 4186 (2006).

⁴ F. E. Pinkerton, M. S. Meyer, G. P. Meisner, and M. P. Balogh, *J. Phys. Chem. B* **110**, 7967 (2006).

⁵ X. Liu, D. Peaslee, and E. H. Majzoub, *J. Mater. Chem. A* **1**, 3926 (2013).

⁶ F. E. Pinkerton, M. S. Meyer, G. P. Meisner, and M. P. Balogh, *J. Alloys Compounds* **433**, 282 (2007).

⁷ M. Matsuo and S.-i. Orimo, *Adv. Energy Mater.* **1**, 161 (2011).

⁸ M. Matsuo, A. Remhof, P. Martelli, R. Caputo, M. Ernst, Y. Miura, T. Sato, H. Oguchi, H. Maekawa, H. Takamura, A. Borgschulte, A. Züttel, and S.-i. Orimo, *J. Am. Chem.*

Soc. **131**, 16389 (2009).

⁹ J. F. Herbst and L. G. Hector, *Appl. Phys. Lett.* **88**, 231904 (2006).

¹⁰ D. J. Siegel, C. Wolverton, and V. Ozoliņš, *Phys. Rev. B* **75**, 014101 (2007).

¹¹ A. Peles and C. G. Van de Walle, *Phys. Rev. B* **76**, 214101 (2007).

¹² G. B. Wilson-Short, A. Janotti, K. Hoang, A. Peles, and C. G. Van de Walle, *Phys. Rev. B* **80**, 224102 (2009).

¹³ S. Hao and D. S. Sholl, *J. Phys. Chem. Lett.* **1**, 2968 (2010).

¹⁴ G. Miceli, C. S. Cucinotta, M. Bernasconi, and M. Parrinello, *J. Phys. Chem. C* **114**, 15174 (2010).

¹⁵ J. Wang, Y. Du, H. Xu, C. Jiang, Y. Kong, L. Sun, and Z.-K. Liu, *Phys. Rev. B* **84**, 024107 (2011).

¹⁶ K. Hoang and C. G. Van de Walle, *Int. J. Hydrogen Energy* **37**, 5825 (2012).

- ¹⁷ K. Hoang and C. G. Van de Walle, *Phys. Rev. B* **80**, 214109 (2009).
- ¹⁸ D. E. Farrell and C. Wolverton, *Phys. Rev. B* **85**, 174102 (2012).
- ¹⁹ K. Hoang, A. Janotti, and C. G. Van de Walle, *Angew. Chem. Int. Ed.* **50**, 10170 (2011).
- ²⁰ J. P. Perdew, K. Burke, and M. Ernzerhof, *Phys. Rev. Lett.* **77**, 3865 (1996).
- ²¹ P. E. Blöchl, *Phys. Rev. B* **50**, 17953 (1994).
- ²² G. Kresse and D. Joubert, *Phys. Rev. B* **59**, 1758 (1999).
- ²³ G. Kresse and J. Hafner, *Phys. Rev. B* **47**, 558 (1993).
- ²⁴ G. Kresse and J. Furthmüller, *Phys. Rev. B* **54**, 11169 (1996).
- ²⁵ G. Kresse and J. Furthmüller, *Comput. Mat. Sci.* **6**, 15 (1996).
- ²⁶ H. J. Monkhorst and J. D. Pack, *Phys. Rev. B* **13**, 5188 (1976).
- ²⁷ G. Henkelman, B. P. Uberuaga, and H. Jónsson, *J. Chem. Phys.* **113**, 9901 (2000).
- ²⁸ C. G. Van de Walle and J. Neugebauer, *J. Appl. Phys.* **95**, 3851 (2004).
- ²⁹ C. Freysoldt, J. Neugebauer, and C. G. Van de Walle, *Phys. Rev. Lett.* **102**, 016402 (2009).
- ³⁰ C. Freysoldt, J. Neugebauer, and C. G. Van de Walle, *phys. status solidi (b)* **248**, 1067 (2011).
- ³¹ X. Wu, D. Vanderbilt, and D. R. Hamann, *Phys. Rev. B* **72**, 035105 (2005).
- ³² M. Gajdoš, K. Hummer, G. Kresse, J. Furthmüller, and F. Bechstedt, *Phys. Rev. B* **73**, 045112 (2006).
- ³³ H. Hemmes, A. Driessen, and R. Griessen, *J. Phys. C: Solid State Phys.* **19**, 3571 (1986).
- ³⁴ Y. E. Filinchuk, K. Yvon, G. P. Meisner, F. E. Pinkerton, and M. P. Balogh, *Inorg. Chem.* **45**, 1433 (2006).
- ³⁵ J. B. Yang, X. J. Wang, Q. Cai, W. B. Yelon, and W. J. James, *J. Appl. Phys.* **102**, 033507 (2007).
- ³⁶ K. Hoang, A. Janotti, and C. G. Van de Walle, *Phys. Rev. B* **85**, 064115 (2012).
- ³⁷ D. E. Farrell, D. Shin, and C. Wolverton, *Phys. Rev. B* **80**, 224201 (2009).
- ³⁸ K. Hoang and M. D. Johannes, *J. Mater. Chem. A* **2**, 5224 (2014).